CHARACTERIZATION OF HEAT TRANSFER AND PRESSURE DROP DURING STEADY STATE FLOW IN PERIODIC OPEN CELULLAR STRUCTURES (POCS)

Dubil K.*, Wetzel T. and Dietrich B.
*Author for correspondence
Institute of Thermal Process Engineering,
Karlsruhe Institute of Technology,
Karlsruhe, Kaiserstrasse 12,
Germany,
E-mail: konrad.dubil@kit.edu

ABSTRACT

Periodic open cellular structures (POCS) are a novel class of structured internals with favorable heat transfer properties and vast design freedom. To exploit their full potential, detailed knowledge of the influence of their geometry on their thermal and hydrodynamic transport properties is required. Therefore, the hypothesis that the heat transfer coefficient and pressure drop of POCS can be described as the superposition of the contributions of their respective strut arrangements is tested. For this purpose, the steady state flow of water through four different versions of cubic POCS is studied with numerical simulations. A comparison between the POCS and their corresponding strut arrangements shows pronounced similarities between the heat transfer and pressure drop in both geometries. This finding is used for the development of new physically founded models for the calculation of the heat transfer coefficient and pressure drop in POCS. They are based on the above-mentioned superposition approach and show a good agreement with the simulation data. Since the models are applicable to arbitrary unit cell geometries, they enable predictive calculations for new unit cell types in the future. Finally, the applicability of an analogy between heat and momentum transfer is tested.

INTRODUCTION

Additive manufacturing offers an enormous flexibility in designing new classes of e.g. mixers, reactors or structured internals [1; 2]. An example of such a new class is the group of periodic open cellular structures (POCS), which consist of a continuous solid and fluid network defined by a periodically repeated unit cell. Their geometry has a strong influence on their thermal and hydrodynamic transport properties making them a promising choice for catalyst carriers in chemical reactors [2; 3] or compact heat exchangers [4]. However, it is essential to have a detailed understanding of this geometrical influence to enable an efficient design process.

For this reason, the convective heat transfer and pressure drop are studied in this contribution. Numerical simulations are used to analyse the steady state flow through four different versions of cubic POCS with varying unit cell dimensions. Their thermal and hydrodynamic properties are compared with unconnected strut arrangements to test the hypothesis that the heat transfer coefficient and pressure drop of POCS can be considered as a superposition of the contributions of their struts. Based on this, physically founded models for both quantities are introduced, which take into account the microstructure of the unit cell.

NOMENCLATURE

A	[m²]	Surface area
C_{Le}	[-]	Lévêque proportionality factor
d	[m]	Diameter of the struts
E	[-]	Error
f_{Proj}	[-]	Projection factor (see Eq. (6))
h	[W/m²/K]	Heat transfer coefficient
Hg	[-]	Hagen number
k	[W/m/K]	Thermal conductivity
L_{B}	[m]	Length of thermal boundary layer
N	[-]	Number
Nu	[-]	Nusselt number
p	[Pa]	Pressure
∇p	[Pa/m]	Pressure gradient
Pr	[-]	Prandtl number
Re	[-]	Reynolds number
s_{L}	[-]	Non-dimensional longitudinal pitch
s_{T}	[-]	Non-dimensional transversal pitch
S_{V}	[m²/m³]	Specific surface area
T	[K]	Temperature
u_0	[m/s]	Superficial velocity
x_{Fric}	[-]	Frictional fraction of total pressure drop

Special characters

ν	[m²/s]	Kinematic viscosity
ρ	[kg/m³]	Density
τ	[Pa]	Shear stress
ϕ	[-]	Temperature coefficient (see Eq. (2))
ψ	[-]	Porosity

Subscripts

Arr	Referring to the strut arrangement
Cell	Referring to the unit cell
F	Referring to the fluid
W	Referring to the solid surface

Additionally, an analogy between heat and momentum transfer is checked. It relates the heat transfer coefficient to frictional forces in the flow and allows prediction of the heat transfer capability based on pressure drop data alone. The proportionality factor of this equation can be used to evaluate the performance of POCS and it is a useful tool for determining the heat transfer coefficient from simpler to perform pressure drop measurements. This approach is motivated by previous work of

our own [4], in which such a relationship was successfully demonstrated for different types of open cellular structures.

GEOMETRY SPECIFICATION

Due to its simplicity, a cubic unit cell was chosen as the starting point of this investigation. However, cubic unit cells are exceptional among POCS because of their channel-like flow properties [4]. To study a broader spectrum of unit cell geometries, which is more representative of other common unit cell types with a more tortuous structure, additional versions of the cubic cell (staggered, inclined and double inclined cubic cells) have been introduced as well. All four unit cells studied in this work are shown in Figure 1.

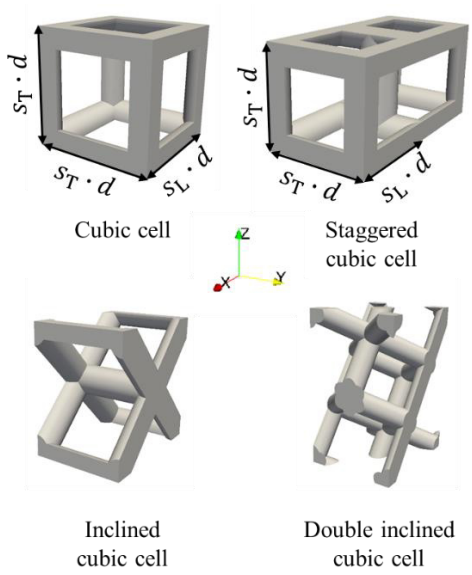

Figure 1 Depiction of the cubic unit cells investigated in this work and definition of longitudinal and transversal pitches

The staggered cubic cell comprises of a regular cubic cell with every second row of its struts being moved by half the unit cell dimension orthogonal to the main flow direction (x-Axis). Rotating the cubic cell 45 degrees about the y-Axis creates the inclined cubic cell. Another rotation about the z-Axis by 35.26 degrees results in the double inclined cubic cell. The definition of the non-dimensional longitudinal s_L and transversal pitches s_T refers to the non-rotated cell, as shown in Figure 1. Their values were varied between $2 \leq s_\mathrm{L} = s_\mathrm{T} \leq 5$ leading to porosities in the range of $59\% < \psi < 92\%$. The diameter of the struts was kept at a constant value of $d = 0.64$ mm. In addition to entire unit cells, unconnected strut arrangements have been studied, as previous work has shown close similarities between the two types of geometries [5], which will also be exploited here.

NUMERICAL METHOD

Numerical simulations were used to analyse the single-phase flow fields in the unit cells mentioned before. The governing conservation equations for mass, momentum and energy were solved using the open source software OpenFOAM. Since this contribution focuses on laminar and steady state flows, its so-called buoyantBoussinesqSimpleFoam solver was utilised with second order discretization schemes. Water was used as the fluid medium with constant physical properties at $T = 305.15$ K resulting in a Prandtl number of $Pr_\mathrm{F} = 5.2$. No buoyancy effects were considered in this work.

The periodicity of the porous structures was exploited to reduce the simulation volume and thus the overall computational effort of the simulations. Two unit cells along and one unit cell orthogonal to the main flow direction were sufficient to achieve a representative elementary volume. By implementing periodic boundary conditions, it became possible to calculate the hydrodynamically and thermally developed flow fields. Conventional periodic boundary conditions were applied on the boundaries orthogonal to the main flow direction, whereas a pressure and temperature gradient are necessary along the stream wise direction to ensure a continuous flow and heat transfer. Hence, boundary conditions were used similar to the suggestions of Beale and Spalding [6]:

$$p_1 = p_2 + \Delta p \tag{1}$$

$$T_1 = (T_2 - T_\mathrm{W}) \cdot \phi + T_\mathrm{W} \tag{2}$$

During the simulation, the pressure drop Δp and temperature coefficient ϕ were iteratively determined to achieve a certain fluid velocity and temperature ($T = 298.15$ K) at the inlet of the simulation volume. A no slip boundary condition and a constant temperature of $T_\mathrm{W} = 313.15$ K were defined on the surface of the solid phase.

Validation of Numerical Models

The impact of the numerical mesh on the target quantities of the simulations was investigated for several different unit cells. The results showed that a base cell size of 53 µm with a refinement by a factor of two near the solid surface and at least three layers led consistently to grid convergence indices [7] below 2 %. The iteration error was estimated with a method proposed by André Martins and Henrique Marchi [8]. By choosing a residual threshold of 10^{-8}, errors lower than 0.1 % were consistently achieved.

Unfortunately, the existing experimental data of POCS is not suitable for validation of the simulation results, since it was generated at higher Reynold numbers and therefore different flow regimes [9; 10]. However, a large number of data and correlations exists for unconnected strut arrangements because of their relevance for the design of shell and tube heat exchangers, which were studied for many decades [11–14]. The literature correlations and simulation results are compared in terms of the non-dimensional Nusselt Nu and Hagen numbers Hg:

$$Nu = \frac{h \cdot L_\mathrm{C}}{k_\mathrm{F}} \qquad \text{with } L_\mathrm{C} = \frac{\pi \cdot d}{2} \tag{3}$$

$$Hg = \frac{\nabla p \cdot L_\mathrm{C}^3}{\rho_\mathrm{F} \cdot \nu_\mathrm{F}^2} \qquad \text{with } L_\mathrm{C} = \frac{\pi \cdot d}{2} \tag{4}$$

The Reynolds number is defined according to Eq. (5):

$$Re = \frac{u_0 \cdot L_\mathrm{C}}{\psi \cdot \nu_\mathrm{F}} \qquad \text{with } L_\mathrm{C} = \frac{\pi \cdot d}{2} \tag{5}$$

The deviations between the simulation results and several correlations for staggered strut arrangements are presented in Figure 2.

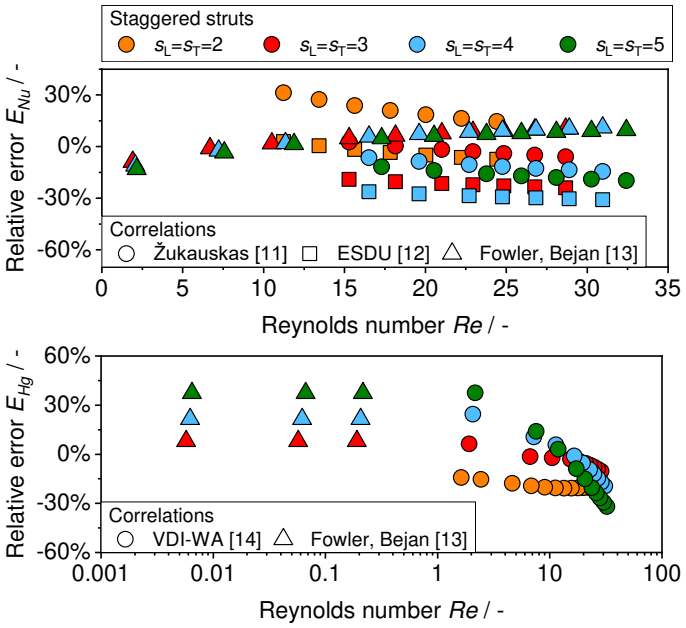

Figure 2 Comparison between Nusselt (top) and Hagen (bottom) numbers obtained from numerical simulations and correlations [11–14]

The simulation data exhibits absolute errors well below 30 % for the convective heat transfer (Nusselt number) and values lower than 40 % for the pressure drop (Hagen number). The mean absolute percentage errors are less than 20 % for each correlation shown, indicating very good agreement. For more details regarding the numerical method and its evaluation, the reader is referred to previous work [5].

HEAT TRANSFER

After validation of the numerical setup, it was used to analyse the convective heat transfer in the cubic unit cells previously depicted in Figure 1. The Reynolds number was varied in a range of $0.001 < Re < 30$, which corresponds to the steady state laminar flow regime. Exemplarily, the data of cells with a non-dimensional pitch of $s_L = s_T = 5$ are shown in Figure 3. The observations described below apply analogously to the other non-dimensional pitches.

All cubic cells exhibit two distinct heat transfer regimes, which directly relate to the state of the thermal boundary layers [4; 5]. With decreasing Reynolds numbers, the boundary layer thickness increases until it reaches the size of the respective cell. In this state, the boundary layer is no longer dependent on the Reynolds number and the heat transfer is dominated by heat conduction (**conduction dominated regime**). As long as the thermal boundary layers are not limited by the size of the cell, their development depends on the flow conditions resulting in the observed variations of the Nusselt numbers at higher Reynolds numbers (**steady state boundary layer dominated regime**). The different slopes of the curves in the second heat transfer regime are attributable to the degree of fluid deflection occurring in each cell. The more tortuous the flow path (see Figure 4), the steeper is the observable curve progression.

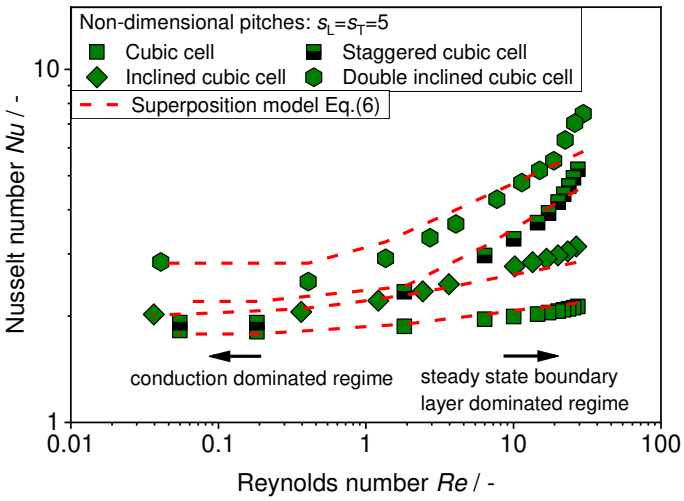

Figure 3 Nusselt number against Reynolds number for all cubic cells studied in this work with $s_L = s_T = 5$. The results obtained from the proposed model (see Eq. (6)) are also shown

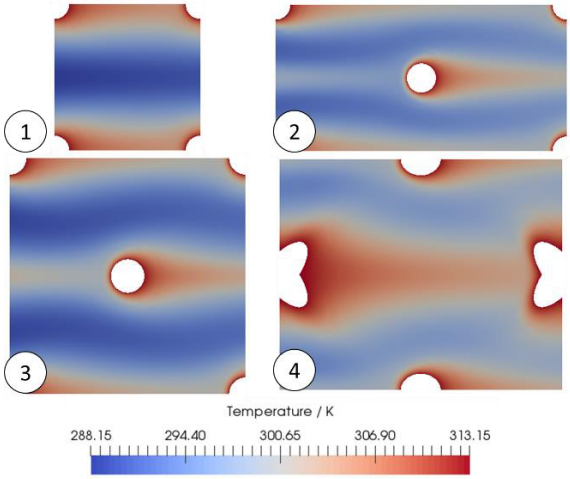

Figure 4 Temperature field for all cubic cells studied in this work with $s_L = s_T = 5$ and a Reynolds number of 10 (1: cubic; 2: staggered cubic; 3: inclined cubic; 4: double inclined cubic)

Interestingly, similar interrelations were found for unconnected strut arrangements with longitudinal and transversal pitches equal to the distances of struts in the POCS. For example, an in-line strut arrangement has a flat Nusselt curve analogous to a cubic cell, whereas a staggered arrangement shows a steeper slope like the staggered cubic cell. Since this observation supports the hypothesis of superposition, an according modelling approach was developed revolving around this concept [5]: Each so-called equivalent strut arrangement present in a unit cell contributes to the overall heat transfer capability of the porous structure proportional to its share of the surface area. Consequently, two-thirds of a cubic unit cell are in-

line struts and one-third inclined struts, which are oriented parallel to the flow. By summing up all contributions, it is possible to model the heat transfer coefficient of the entire unit cell resulting in Eq. (6):

$$Nu_{\mathrm{Cell}} = \sum_{i=1}^{N_{\mathrm{Arr}}} Nu_i \cdot \frac{A_i}{A_{\mathrm{Cell}}} \cdot f_{\mathrm{Proj},i} \qquad (6)$$

Additional effects caused by junctions of struts were considered by reducing the surface of the respective strut arrangement A_i. Furthermore, a projection factor $f_{\mathrm{Proj},i}$ had to be introduced for inclined struts. A detailed description of the model and its derivation is provided in [5]. The modelling results for each cubic POCS geometry with non-dimensional pitches of $s_{\mathrm{L}} = s_{\mathrm{T}} = 5$ are included in Figure 3. The model is able to capture both heat transfer regimes and adequatly describes the different slopes in the steady state boundary layer dominated regime. Larger deviations are only visible for the staggered and double inclined cubic cells at the highest Reynolds numbers. These can be attributed to a changing velocity distribution in the POCS, which has no counterpart in the unconnected strut arrangements [5]. Nonetheless, the superposition model shows a very good agreement with the simulation results resulting in a mean average percentage error below 15 %.

PRESSURE DROP

Analogous to the convective heat transfer, the influence of the unit cell geometry on the pressure drop was investigated. Typically, pressure drop data in porous media is described with Ergun-Type [15] equations, which superimpose the so-called Darcy and Forchheimer regimes:

$$Hg = C_1 \cdot Re + C_2 \cdot Re^2 \qquad (7)$$

Within the Darcy regime, the pressure drop is linearly dependent on the Reynolds number due to the predominance of viscous forces in the flow. At higher Reynolds numbers, inertial forces become relevant, which exhibit a quadratic relationship between pressure drop and Reynolds number. To better distinguish both regimes, it is useful to plot the quotient of the Hagen and Reynolds number against the Reynolds number, as shown in Figure 5 for all cubic cell versions with non-dimensional pitches of $s_{\mathrm{L}} = s_{\mathrm{T}} = 5$.

The Darcy and Forchheimer regimes are easily discernible by the changing slopes observed in Figure 5. All cells remain in the Darcy regime up to a Reynolds number of roughly $Re \approx 1$ and show similar absolute values of the pressure drop. Although each cubic cell has a different microstructure considering the main flow direction, their averaged geometric quantities like the porosity and specific surface area are the same. Apparently, the impact of the microstructure is very limited in the Darcy regime, whereas large differences are observable in the Forchheimer regime. The more tortuous the solid structure of the porous medium, the higher is the pressure drop and slope in Figure 5. This agrees well with the experimental results of Klumpp et al. [10], who investigated the flow through cubic cells with different orientations to the flow at even larger Reynolds numbers. Consequently, inertial forces appear to have a more pronounced dependency on the geometric structure of the unit cell than viscous forces. Nonetheless, none of the curves reaches a slope of one (staggered and double inclined cubic cells exhibit a slope of approximately 0.5) indicating that viscous forces are still relevant within the steady state laminar regime.

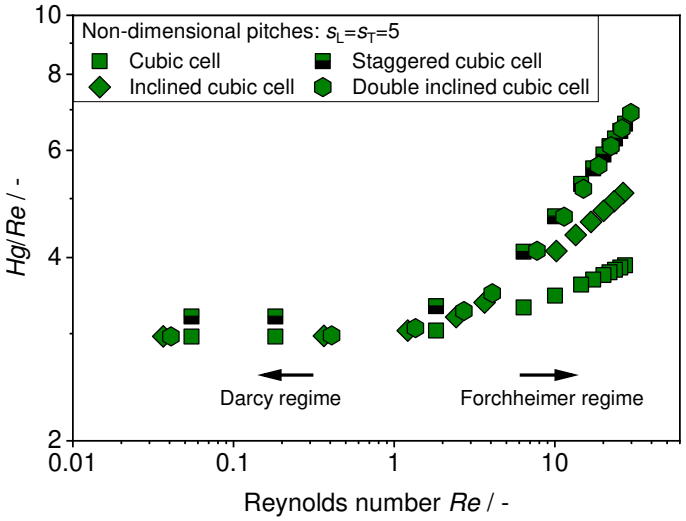

Figure 5 Quotient of Hagen and Reynolds number against Reynolds number for different unit cells with $s_{\mathrm{L}} = s_{\mathrm{T}} = 5$

Corresponding observations were made for unit cells with smaller non-dimensional pitches, as exemplarily shown for a cubic and staggered cubic cell in Figure 6. A reduction of the unit cell dimension does not alter the curve progression, but it significantly increases the pressure drop, as the porosity of the unit cells is also reduced. This antiproportional relationship between porosity and pressure drop is common amongst porous media and was also observed for POCS by other authors [9; 10].

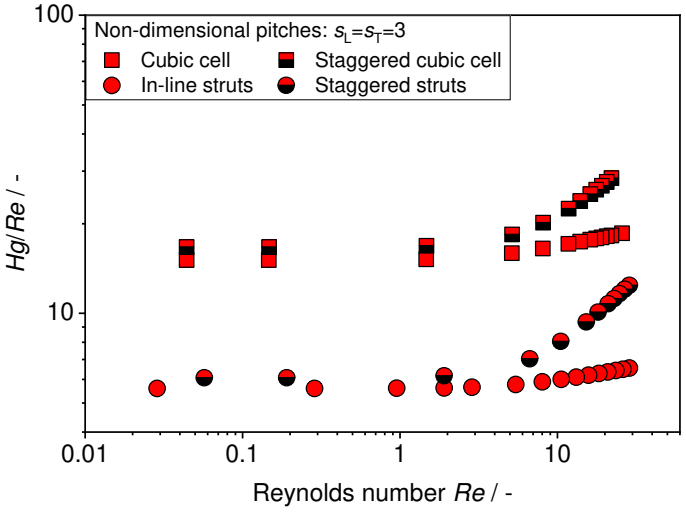

Figure 6 Comparison of the non-dimensional pressure drop between cubic cells and their corresponding strut arrangements

In addition to POCS, the pressure drop of two of their equivalent strut arrangements are shown in Figure 6. Although the absolute values of the pressure drop differ, the curve

progressions of the in-line and the staggered structures are very similar in each case. Since this observation is analogous to the findings related to the heat transfer, the superposition hypothesis is also tested for the pressure drop. In contrast to the heat transfer coefficient, the pressure drop is related to the length of the unit cell along the stream wise direction instead of the surface area, when the Hagen number is used (see Eq. (4)). Therefore, it is sufficient to sum up the contributions of all the equivalent strut arrangements [5], which each flow path encounters throughout the unit cell. This leads to the following model equation:

$$Hg_{\mathrm{Cell}} = \sum_{i=1}^{N_{\mathrm{Arr}}} Hg_i \cdot N_i \tag{8}$$

The number of each strut arrangement N_i on a flow path is one for all unit cells except for the cubic cell. In this case, the flow passes through two in-line and one inclined arrangement. To make use of Eq. (8), mathematical functions for the non-dimensional pressure drop Hg_i are necessary. Therefore, the simulation data was utilized to derive a fit function in the form of Eq. (7) for each equivalent strut arrangement. The porosity, which is necessary for the determination of the Reynolds number, was calculated according to the following equation:

$$\psi_{\mathrm{Arr}} = 1 - \frac{\pi}{4 \cdot s_{\mathrm{T}}} \tag{9}$$

A comparison of the new pressure drop model with the simulation results of the POCS is provided in Figure 7.

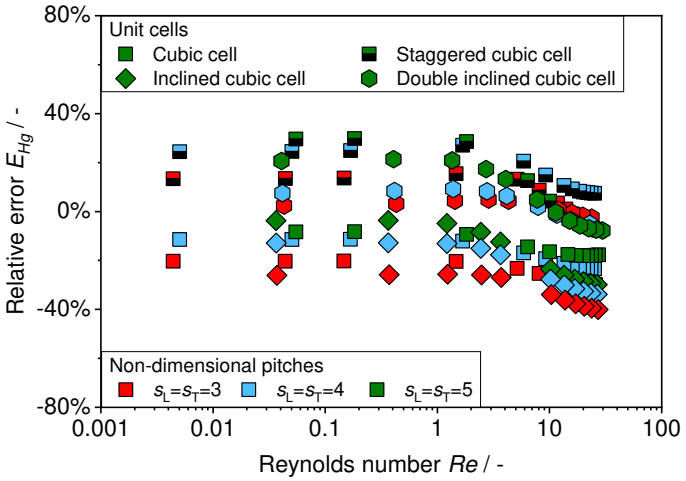

Figure 7 Comparison between Hagen numbers obtained from numerical simulations and values calculated with Eq. (8)

The proposed model shows a good agreement with the simulation data over the entire investigated range of Reynolds numbers with a mean average percentage error of 16 % and a maximum absolute error of 40 %. The highest deviations are observable for the inclined cubic cell, whereas the lowest absolute errors are achieved for the double inclined cubic cell. In the Forchheimer regime ($Re > 1$), the impact of the non-dimensional pitches becomes apparent: The larger the pitches, the lower is the deviation between model and simulation. POCS with non-dimensional pitches of $s_{\mathrm{L}} = s_{\mathrm{T}} = 2$ exhibited the largest absolute errors with outliers reaching values of 80 %. Therefore, they were excluded from the comparison restricting the validity range of the model and the underlying superposition hypothesis to POCS with higher porosities ($3 \leq s_{\mathrm{L}} = s_{\mathrm{T}} \leq 5$).

ASSESSMENT OF THE ANALOGY BETWEEN HEAT AND MOMENTUM TRANSFER

The Generalized Lévêque Equation (GLE) provides a useful analogy between the shear stress and the convective heat transfer in various internal and external flow problems [16]. Its integral form (see Eq. (10)) was tested by Meinicke et al. [4] for open cellular structures, including irregular sponges as well as four POCS geometries.

$$h = C_{\mathrm{Le}} \cdot \sqrt[3]{\frac{\tau \cdot Pr_{\mathrm{F}} \cdot \rho_{\mathrm{F}} \cdot k_{\mathrm{F}}^3}{(\rho_{\mathrm{F}} \cdot \nu_{\mathrm{F}})^2 \cdot L_B}} \tag{10}$$

Meinicke et al. [4] defined the thermal boundary layer length as $L_{\mathrm{B}} = \pi \cdot d/2$ following established suggestions for the flow around cylinders [14]. The shear stress can be replaced with the frictional fraction of the pressure gradient divided by the specific surface area ($\tau = x_{\mathrm{Fric}} \cdot \nabla p / S_{\mathrm{V}}$) leading to the following non-dimensional relation for the Nusselt number:

$$Nu = C_{\mathrm{Le}} \cdot \sqrt[3]{x_{\mathrm{Fric}} \cdot Hg \cdot Pr_{\mathrm{F}} \cdot \frac{2}{S_{\mathrm{V}} \cdot \pi \cdot d}} \tag{11}$$

Based on the simulation data, the proportionality factor of the GLE was determined for the cubic unit cells studied in this work. The results are presented in Figure 8.

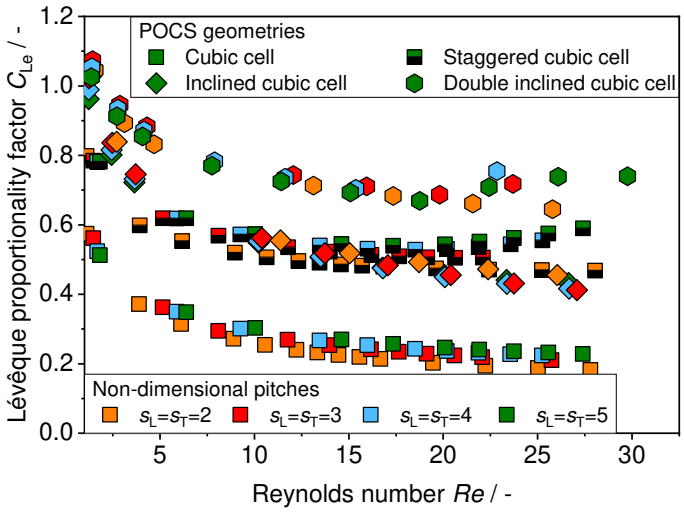

Figure 8 Lévêque proportionality factor against Reynolds number for different cubic cells and non-dimensional pitches

For the analogy to be valid and applicable, the Lévêque proportionality factor should approach a constant value, which is the case for larger Reynolds numbers. However, it grows as the Reynolds number decreases: The Nusselt number reaches a constant value above zero (see Figure 3), whereas the lower limit of the Hagen number is exactly this value. Consequently, the proportionality factor approaches infinity. Following the derivation of this analogy, it is only logical that its applicability is restricted to higher Reynolds numbers. It assumes that the

thermal boundary layers are much smaller than the hydrodynamic ones necessitating boundary layer reformation instead of fully developed boundary layers.

Regarding the absolute values of the proportionality factor, large differences between the unit cell geometries are observable. The double inclined cubic cell exhibits the highest values indicating a favourable relation between convective heat transfer and frictional pressure drop. Staggered and inclined cubic cells have similar but lower values. However, the cubic unit cells show by far the smallest proportionality factors. Considering the influence of the non-dimensional pitches, no definite trend can be derived from the data available. In contrast, the ratio between the Nusselt and Hagen number increases monotonically with growing non-dimensional pitches for all cubic POCS studied. The geometrical influence of the unit cell on this ratio follows the same trend as the proportionality factor.

For sufficiently high Reynolds numbers, the GLE enables the derivation of convective heat transfer coefficients from pressure drop measurements that are simpler to perform. However, to take full advantage of this analogy, further research is needed to determine the relationship between the unit cell geometry and the corresponding Lévêque proportionality factor.

CONCLUSION

Numerical simulations of the steady state flow of water through heated periodic open cellular structures (POCS) with an isothermal boundary condition were carried out. The convective heat transfer and pressure drop were studied for four versions of cubic POCS with non-dimensional pitches in the range of $2 \leq s_L = s_T \leq 5$. Two different regimes were observed for both heat transfer and pressure drop, each having different functional relationships between the corresponding non-dimensional number and the Reynolds number. The unit cell geometry has a strong impact on the results, especially at higher Reynolds numbers. The more tortuous its geometry, the higher are the Nusselt and the Hagen numbers in the steady state boundary layer dominated and Forchheimer regimes, respectively. An increase of the non-dimensional pitches reduces both quantities but has a negligible effect on the overall curve progressions.

To test the hypothesis that the heat transfer coefficient and pressure drop of POCS can be described as the superposition of their struts, their thermal and hydrodynamic transport properties were compared with those of unconnected strut arrangements with corresponding geometries, which are referred to as equivalent strut arrangements. Since close similarities were observed, a new modelling approach was established that revolves around this concept of superposition. It adds up the contributions of all equivalent strut arrangements and shows a good agreement with the simulation results for geometries with $s_L = s_T \geq 3$, supporting the proposed superposition hypothesis. The models are very flexible and can be adapted to new unit cell geometries, enabling predictive calculations and facilitating an efficient design process of POCS in the future.

Finally, the applicability of an analogy between heat and momentum transport was tested. It is valid for all geometries studied, but only at higher Reynolds numbers when a reformation of the hydrodynamic and thermal boundary layers is achieved. In such cases, this analogy is a useful tool to calculate convective heat transfer coefficients from easier to obtain pressure drop data.

REFERENCES

[1] C. Parra-Cabrera, C. Achille, S. Kuhn, R. Ameloot, 3D printing in chemical engineering and catalytic technology, Structured catalysts, mixers and reactors, Chemical Society reviews 47 (1) (2018) 209–230.

[2] C. Busse, H. Freund, W. Schwieger, Intensification of heat transfer in catalytic reactors by additively manufactured periodic open cellular structures (POCS), Chemical Engineering and Processing: Process Intensification 124 (2018) 199–214.

[3] L. Fratalocchi, C. Giorgio Visconti, G. Groppi, L. Lietti, E. Tronconi, Intensifying heat transfer in Fischer-Tropsch tubular reactors through the adoption of conductive packed foams, Chemical Engineering Journal 349 (2018) 829–837.

[4] S. Meinicke, K. Dubil, T. Wetzel, B. Dietrich, Characterization of heat transfer in consolidated, highly porous media using a hybrid-scale CFD approach, International Journal of Heat and Mass Transfer 149 (2020) 119201.

[5] K. Dubil, T. Wetzel, B. Dietrich, Modelling steady-state convective heat transfer in different periodic open cellular structures (POCS) - A superposition approach, submitted to International Journal of Heat and Mass Transfer (2022).

[6] S. B. Beale, D. B. Spalding, Numerical study of fluid flow and heat transfer in tube banks with stream-wise periodic boundary conditions, Transactions of the CSME 22 (4A) (1998) 397–416.

[7] P. J. Roache, Perspective: A Method for Uniform Reporting of Grid Refinement Studies, Journal of Fluids Engineering 116 (3) (1994) 405.

[8] M. André Martins, C. Henrique Marchi, Estimate of Iteration Errors in Computational Fluid Dynamics, Numerical Heat Transfer, Part B: Fundamentals 53 (3) (2008) 234–245.

[9] N. F. Bastos Rebelo, K. Anne Andreassen, L. I. Suarez Ríos, J. C. Piquero Camblor, H.-J. Zander, C. A. Grande, Pressure drop and heat transfer properties of cubic iso-reticular foams, Chemical Engineering and Processing: Process Intensification 127 (2018) 36–42.

[10] M. Klumpp, A. Inayat, J. Schwerdtfeger, C. Körner, R. F. Singer, H. Freund, W. Schwieger, Periodic open cellular structures with ideal cubic cell geometry, Effect of porosity and cell orientation on pressure drop behavior, Chemical Engineering Journal 242 (2014) 364–378.

[11] A. Žukauskas, Heat transfer from tubes in crossflow, in: Advances in heat transfer, Elsevier, Amsterdam (1972) 93–160.

[12] Engineering Sciences Data Unit, Convective heat transfer during crossflow of fluids over plain tube banks, ESDU Data Item No. 73031, London (1973).

[13] A. J. Fowler, A. Bejan, Forced convection in banks of inclined cylinders at low Reynolds numbers, International Journal of Heat and Fluid Flow 15 (2) (1994) 90–99.

[14] Verein Deutscher Ingenieure, VDI-Wärmeatlas, Springer Vieweg, Berlin, Heidelberg (2013).

[15] S. Ergun, A. A. Orning, Fluid Flow through Randomly Packed Columns and Fluidized Beds, Industrial & Engineering Chemistry 41 (6) (1949) 1179–1184.

[16] H. Martin (2005), The Léveque-Analogy or how to predict heat and mass-transfer from fluid friction, HEFAT 2005, 4th International Conference on Heat Transfer, Fluid Mechanics and Thermodynamics, September 19 - 22, 2005, Cairo, Egypt.